Silver-Functionalized AlGaN/GaN Heterostructure Diode for Ethanol Sensing

Sunwoo Jung,[a,*] Kwang Hyeon Baik,[b] Fan Ren,[c,] S. J. Pearton,[d,**] and Soohwan Jang[a,***,z]**

[a]*Department of Chemical Engineering, Dankook University, Yongin 16890, Korea*
[b]*School of Materials Science and Engineering, Hongik University, Jochiwon, Sejong 30016, Korea*
[c]*Department of Chemical Engineering, University of Florida, Gainesville, Florida 32611, USA*
[d]*Department of Materials Science and Engineering, University of Florida, Gainesville, Florida 32611, USA*

The use of Ag in the gate region of AlGaN/GaN heterostructure diodes is shown to provide stable, reversible changes in barrier height and thus current during exposure to ethanol at 250°C. The exposed ethanol molecules are adsorbed on the silver and oxidized, resulting in the increase of Schottky barrier height. The detection limit of ethanol at this temperature was 58 ppm, and the sensor response was linear over the range 58–58700 ppm. For the high end of this concentration range (5.87%), ethanol exposure at 250°C caused the Schottky barrier height to change from 0.604 eV to 0.656 eV, which produced a forward current relative change of 45.4% at 0.9V forward bias. The results are competitive with detection of ethanol by oxide thin films or nanostructures of SnO_2, Fe_2O_3, CuO, and ZnO.

Manuscript submitted March 15, 2017; revised manuscript received May 26, 2017. Published July 7, 2017.

There are many applications in which detection of the common aliphatic alcohol, ethanol, is needed, including the chemical, biomedical, and food industries, where the rate of ethanol production during fermentation needs to be monitored.[1] As an example, the change in alcohol content during fermentation of grapes is of great importance in the winemaking industry.[2] Ethanol gas sensors can detect early spoilage of carbohydrate-rich foods, and these sensors are now employed in consumer electronics including refrigerators and mobile devices.[1] Another common application is monitoring blood alcohol content related to consumption of alcoholic beverages. Most of the research into solid state sensors has focused on metal oxide semiconductors such as SnO_2, Fe_2O_3, CuO, and ZnO.[3–31] The attractive features of semiconductor-based sensors include that they can be operated with fast response at low power consumption and with compact size.[32–36]

The AlGaN/GaN heterostructure materials system is an attractive one for sensors since it allows robust high temperature operation in harsh environments.[37–41] Many types of GaN based devices have been reported for gas and chemical sensing, including Schottky diodes, metal oxide semiconductor (MOS) diodes, and AlGaN/GaN high electron mobility transistors (HEMTs). The specificity of the sensors can be tailored by the choice of the gate material, which might include antibody layers for biological species detection or catalytic metals for gas sensing.[42,43] In particular, the AlGaN/GaN HEMT structure with its two dimensional electron gas (2-DEG) channel induced by piezoelectric and spontaneous polarization at the interface between the AlGaN and GaN layers shows highly sensitive current changes to surface charges created by catalytic reaction of target gases on the specific active sensing layer. With 30% Al concentration in the AlGaN layer, 5∼10 times higher channel sheet electron densities are obtained compared to GaAs or InP HEMTs.

In this study, AlGaN/GaN HEMT based Schottky diode ethanol sensors using silver as a sensing material were fabricated, and the response of the devices to ethanol gas was investigated as a function of temperature and ethanol concentration. The diodes showed a current reduction in ethanol-containing ambients due to the increase of Schottky barrier height. This process was most efficient at 250°C, and rapid responses to cyclic exposures of various concentrations of ethanol gas were obtained.

Experimental

AlGaN/GaN HEMT layer structures were grown on *c-plane* sapphire by metal organic chemical vapor deposition (MOCVD). The epilayer structures were composed of 2 μm thick undoped GaN buffer layer followed by a 35 nm unintentionally doped $Al_{0.3}Ga_{0.7}N$ layer. Sheet resistances of 350 ohm/square, sheet carrier concentrations of 1.06×10^{13} cm^2, and mobilities of 1900 cm^2/Vs were obtained from Hall measurements. ohmic contacts of Ti/Al/Ni/Au were formed by E-beam evaporator and lift-off, and annealed at 900°C for 60 s under a N_2 ambient. A 200 nm SiN_x layer was deposited for diode isolation by plasma enhanced chemical vapor deposition (PECVD). The windows for active area opening were achieved by buffered oxide etchant (BOE) etching. A 10 nm Ag film was deposited on the diode Schottky contact area by E-beam evaporation. Finally, Ti/Au based contact pads were deposited for probing and wire bonding. Figure 1 shows the layer structure and geometry, and the microscopic image of the sensor. Current-voltage (I-V) characteristics of the Schottky diodes were measured at 25–300°C using an Agilent 4156C parameter analyzer with the diodes in a gas test chamber in ambients of N_2 bubbled through ethanol to produce controlled concentrations of 58–58700 ppm (0.00578–5.87% by volume). Figure 2 shows a schematic of the test setup. The temperature of the sensors could be controlled from 25–300°C and dry N_2 was used to transport ethanol vapor to the sensor surface.

Results and Discussion

Figure 3a shows the I-V characteristics from the Ag-AlGaN/GaN diode in dry N_2 or during exposure to 5.87% ethanol in N_2 at 250°C. The current decreases, consistent with an increase in the effective Schottky barrier height and this is more obvious at forward bias voltages, as is normal for gas sensing with nitride-based sensors.[42,43] The relative current change as a function of bias is shown in Figure 3b. The response is largest (45.4%) at a forward bias of 0.9 V.

The barrier height could be measured from the I-V characteristic during the period that ethanol was present on the sensor surface and compared to its value when N_2 was the ambient in the test chamber. The barrier height (Φ_b) was then extracted from the relationship between current density J, temperature T and applied voltage V

$$J = A^* T^2 \exp\left(\frac{-e\phi_b}{kT}\right) \exp\left(\frac{eV}{nkT}\right)$$

where A^* is Richardson's constant, k is Boltzmann's constant, e is the electronic charge, and n is the diode ideality factor.[36,40,41] Figure 4 shows the value of barrier height as 5.87% ethanol is introduced and

*Electrochemical Society Student Member.
**Electrochemical Society Fellow.
***Electrochemical Society Active Member.
[z]E-mail: jangmountain@dankook.ac.kr

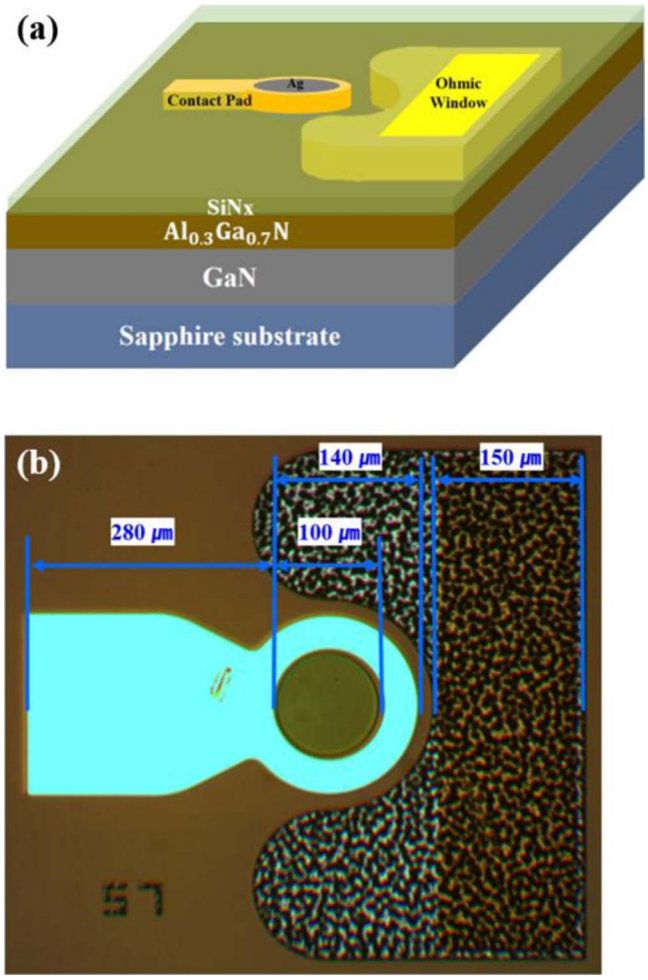

Figure 1. (a) Layer structure and geometry of the Ag-AlGaN/GaN diode sensor of the completed device. The circular Ag Schottky contact is surrounded by the ohmic contact. (b) Top-view microscopic image of the device with dimensions.

nitrogen is switched back to the test chamber with the diode held at 250°C. The barrier height increases by 0.053 eV to 0.656 eV.

In contrast to the hydrogen detection of AlGaN/GaN heterostructure diode using Pt as a catalytic Schottky electrode, the barrier height was increased upon ethanol exposure.[33–37,40,41,44–46] The possible mechanism for the current decrease due to barrier height increase can be described as follows. Firstly, there is adsorption of ethanol molecules onto the silver surface on the gate of the diode. The adsorption of ethanol molecules can be enhanced by adsorbed oxygen ions on silver, which are induced from the decomposition of silver oxide (Ag_2O) formed during the device fabrication process.[47,48] It is notable that both the formation of oxygen ion and decomposition

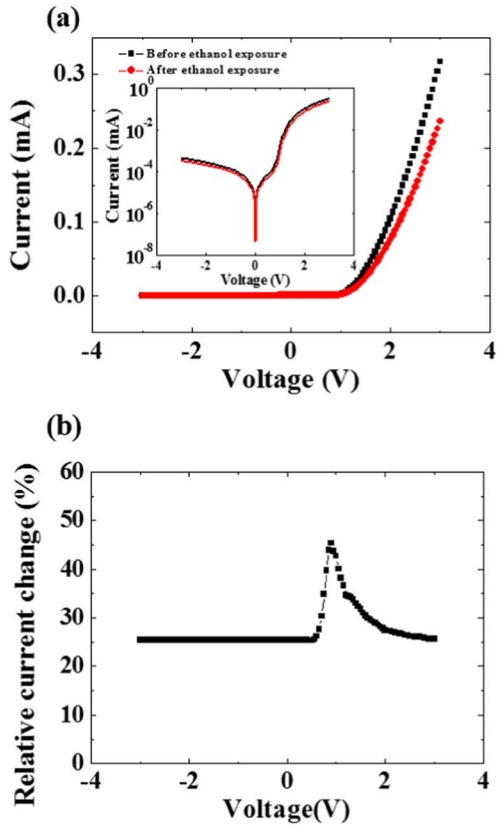

Figure 3. (a) I-V characteristics from the Ag-AlGaN/GaN diode in dry N_2 or during exposure to 5.87% ethanol in N_2 at 250°C. The inset is the semi-log plot of I-V. (b) Relative current change as a function of bias.

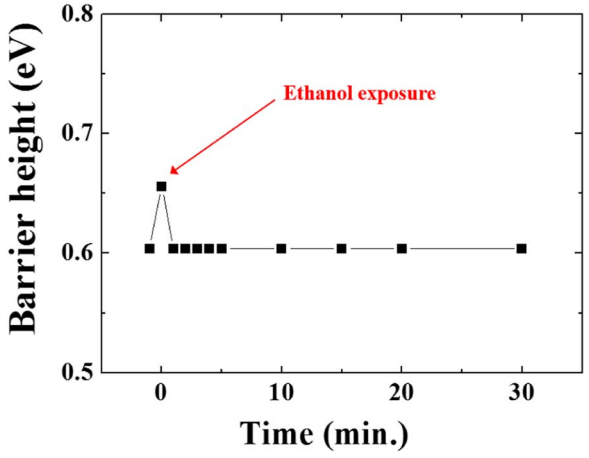

Figure 4. Change in effective barrier height as a function of time for an injection of ethanol gas into the test chamber, followed by a return to dry N_2.

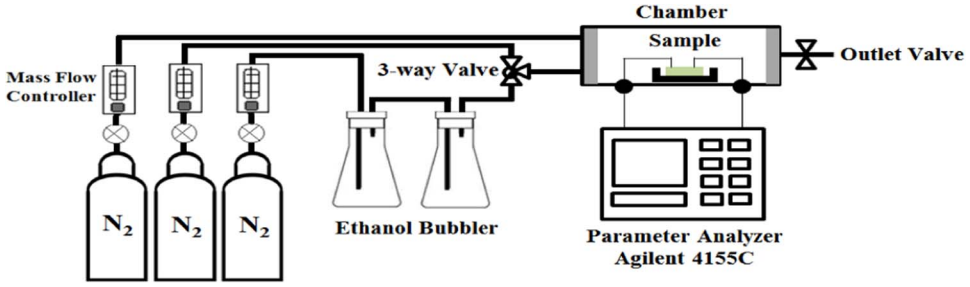

Figure 2. Schematic of ethanol testing setup.

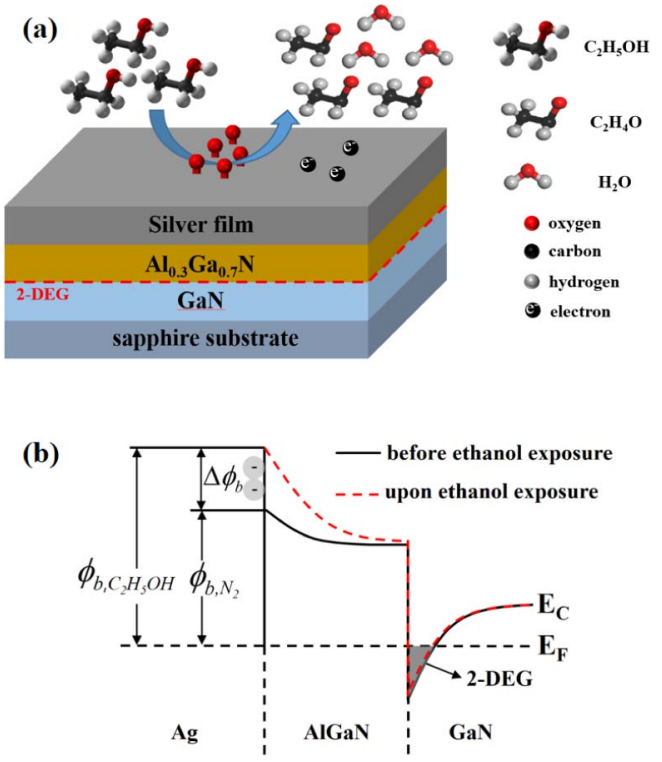

Figure 5. (a) Schematic of oxidation of ethanol on Ag in the gate region of the diode. (b) Energy band diagram of Ag Schottky barrier on AlGaN/GaN structure, E_c: conduction band edge, E_F: Fermi level, ϕ_{b,C_2H_3OH}, ϕ_{b,N_2}: Schottky barrier heights in ethanol and nitrogen ambient respectively, and $\Delta\phi_b$: Schottky barrier height increase.

of Ag_2O occur above 200°C.[49–51] The silver on the semiconductor surface enhances the catalytic oxidation of alcohol gas.[47,49,52] The adsorbed ethanol molecules react with oxygen ions to produce C_2H_4O, H_2O, and electrons. Hence, this reaction causes negative charging of silver electrode, resulting in the Schottky barrier height increase. Finally, this increase of Schottky barrier height induces a decrease in current at both forward and reverse bias. The reaction and the energy band diagram of Ag Schottky barrier on AlGaN/GaN structure upon ethanol exposure are shown schematically in Figure 5. The overall reaction is:

$$C_2H_5OH + O^- \rightarrow C_2H_4O + H_2O + e^-$$

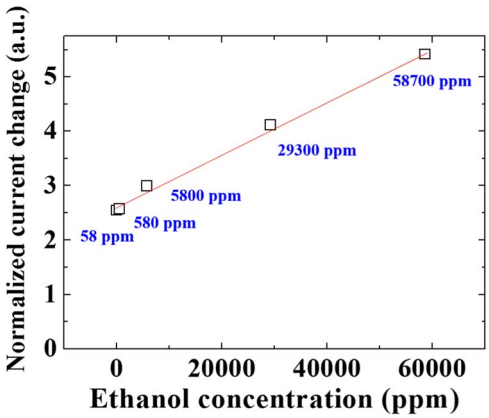

Figure 6. Normalized current change in Ag-AlGaN/GaN diodes as a function of ethanol concentration at 250°C.

The current change was measured as a function of ethanol concentration at 250°C. Figure 6 shows that the current response was linear over the range 58–58700 ppm at this temperature. We should point out that at temperatures below 250°C, there was not a significant change in diode current upon exposure to ethanol, while at 300°C, the response was slightly lower than at 250°C, which may be due to additional reactions of the Ag with the semiconductor. Many country's legal limit for blood alcohol content of automobile drivers is 0.05%, corresponding to 0.01% (100 ppm) breath alcohol content. Any measurable alcohol in the blood is mostly illegal in U. S. These sensors are easily able to detect these types of concentrations.

Table I shows a comparison of ethanol detection sensitivities for different oxide-based material systems involving either thin films or nanostructures.[10–17] Note that the operating temperature and sensitivity of the Ag-AlGaN/GaN diodes is competitive with most of the other technologies. Among the potential advantages of the nitride-based diodes is the ease of array fabrication to integrate other types of sensors or use of diode pairs in which one diode is sensitive to temperature changes but not ethanol.[42] Finally, these types of sensors are easily integrated with wireless data transmission circuits for remote monitoring applications.[42]

Conclusions

The Ag-AlGaN/GaN diodes showed maximum sensitivity to ethanol at 250°C, and stable and recoverable response to ethanol vapor resulting from reversible changes in barrier height. The barrier height increase for ethanol vapor exposure at 250°C was 0.053 eV for the thin silver film Schottky diode. The diodes showed a rapid

Table I. Summary of ethanol detection limits and operating temperatures for Ag-AlGaN/GaN and different oxide-based materials.[9–17]

	Sensing material	Material Structure	Limit of detection (ppm)	Detection range (ppm)	Measurement temperature (°C)	Sensitivity (%)	Concentration used for sensitivity (ppm)
This Study	Ag/AlGaN/GaN HEMT	film	58	58–58721	250	45	58721
Ref. 9	Pd/ZnO	nanorods	190	190–1530	200	94	1530
Ref. 10	Sm_2O_3/ZnO	nano-flower	10	10–500	300	97*	500
Ref. 11	CO_3O_4/TiO_2	nanorods	100	100	260	3900*	100
Ref. 12	V_2O_5	nano-urchin	5	5–1000	250	88*	1000
Ref. 13	Au/V_2O_5	nanotube	100	100–500	220	1700*	100
Ref. 14	Graphene/ITO	nanocomposite	50	50–1000	350	100*	1000
Ref. 15	SnO_2	quantum dot	50	50	200	2900*	50
Ref. 16	CuO	nano-flower	100	100	300	600*	100
Ref. 17	Pt/SnO_2	hollow nanosphere	0.25	0.25–5	325	100*	5

*Sensitivity has been re-calculated with the definition of $\frac{r_{ref}-r_{ethanol}}{r_{ref}} \times 100\%$ from the literature. The r_{ref} and $r_{ethanol}$ are resistances in the reference and ethanol gases respectively.

sensing response to ethanol, as well as a full recovery to their initial current level after removing the ethanol from the ambient. This study shows the possibility of AlGaN/GaN HEMT with active silver layer to ethanol sensing to monitor food spoilage, drunk driving, and alcohol levels in many industrial applications.

Acknowledgments

This research was supported by Basic Science Research Program through the NRF of Korea (2017R1D1A3B03035420, 2015R1D1A1A01058663), and Nano · Material Technology Development Program through the NRF of Korea (2015M3A7B7045185). The work at UF was partially supported by HDTRA1-17-1-0011.

References

1. J. Banerjee, R. Singh, R. Vijayaraghavan, D. MacFarlane, A. F. Patti, and A. Arora, *Food Chem.*, **225**, 10 (2017).
2. F. Jiménez-Márquez, J. Vázquez, J. Úbeda, J. Rodríguez-Rey, and J. L. Sánchez-Rojas, *Proc. SPIE*, **9517**, 95171P (2015).
3. J. T. S. Allan, M. R. Rahman, and E. B. Easton, *Sens. Actuators, B*, **239**, 120 (2017).
4. D. Sebők, L. Janovák, D. Kovács, A. Sápi, D. G. Dobó, Á. Kukovecz, Z. Kónya, and I. Dékány, *Sens. Actuators, B*, **243**, 1205 (2017).
5. F. H. Saboor, A. A. Khodadadi, Y. Mortazavi, and M. Asgari, *Sens. Actuators, B*, **238**, 1070 (2017).
6. F. A. Harraz, A. A. Ismail, S. A. Al-Sayari, A. Al-Hajry, and M. S. Al-Assiri, *Superlattices Microstruct.*, **100**, 1064 (2016).
7. M. Tonezzer, T. T. L. Dang, Q. H. Tran, and S. Iannotta, *Sens. Actuators, B*, **236**, 1011 (2016).
8. X. Yang, S. Tian, R. Li, W. Wang, and S. Zhou, *Sens. Actuators, B*, **241**, 210 (2017).
9. S. Roy, N. Banerjee, C. K. Sarkar, and P. Bhattacharyya, *Solid-State Electron.*, **87**, 43 (2013).
10. M. Bagheri, N. F. Hamedani, A. R. Mahjoub, A. A. Khodadadi, and Y. Mortazavi, *Sens. Actuators, B*, **191**, 283 (2014).
11. Y. Q. Liang, Z. D. Cui, S. L. Zhu, Z. Y. Li, X. J. Yang, Y. J. Chen, and J. M. Ma, *Nanoscale*, **5**, 10916 (2013).
12. Y. Qin, G. Fan, K. Liu, and M. Hu, *Sens. Actuators, B*, **190**, 141 (2014).
13. W. Zeng, W. Chen, Z. Li, H. Zhang, and T. Li, *Mater. Res. Bull.*, **65**, 157 (2015).
14. K. Inyawilert, A. Wisitaoraat, C. Sriprachaubwong, A. Tuantranont, S. Phanichphant, and C. Liewhiran, *Sens. Actuators, B*, **209**, 40 (2015).
15. Y. He, P. Tang, J. Li, J. Zhang, F. Fan, and D. Li, *Mater. Lett.*, **165**, 50 (2016).
16. A. Umar, J. Lee, R. Kumar, O. Al-Dossary, A. A. Ibrahim, and S. Baskoutas, *Mater. Des.*, **105**, 16 (2016).
17. B. Kim, J. S. Cho, J. Yoon, C. W. Na, C. Lee, J. H. Ahn, Y. C. Kang, and J. Lee, *Sens. Actuators, B*, **234**, 353 (2016).
18. S. M. Chou, L. G. Teoh, W. H. Lai, Y. H. Su, and M. H. Hon, *Sensors*, **6**, 1420 (2006).
19. Y. Chen, X. Li, X. Li, J. Wang, and Z. Tang, *Sens. Actuators, B*, **232**, 158 (2016).
20. Z. Qiang, S. Y. Ma, H. Y. Jiao, T. T. Wang, X. H. Jiang, W. X. Jin, H. M. Yang, and H. Chen, *Ceram. Int.*, **42**, 18983 (2016).
21. J. Tan, J. Chen, K. Liu, and X. Huang, *Sens. Actuators, B*, **230**, 46 (2016).
22. M. Mitsushio, T. Masunaga, T. Yoshidome, and M. Higo, *Prog. Org. Coat.*, **91**, 33 (2016).
23. C. Hsu, J. Tsai, and T. Hsueh, *Sens. Actuators, B*, **224**, 95 (2016).
24. Y. He, P. Tang, J. Li, J. Zhang, F. Fan, and D. Li, *Mater. Lett.*, **165**, 50 (2016).
25. P. Rao, R. V. Godbole, and S. Bhagwat, *J. Magn. Magn. Mater.*, **416**, 292 (2016).
26. S. Yang, Y. Liu, T. Chen, W. Jin, T. Yang, M. Cao, S. Liu, J. Zhou, G. S. Zakharova, and W. Chen, *Appl. Surf. Sci.*, **393**, 377 (2017).
27. Q. Wan, Q. H. Li, Y. J. Chen, T. H. Wang, X. L. He, J. P. Li, C. , and L. Lin, *Appl. Phys. Lett.*, **84**, 3654 (2004).
28. M. Ben Amor, A. Boukhachem, A. Labidi, K. Boubaker, and M. Amlouk, *J. Alloys Compd.*, **693**, 490 (2017).
29. S. Blanco, R. Vargas, J. Mostany, C. Borrás, and B. R. Scharifker, *J. Electroanal. Chem.*, **740**, 61 (2015).
30. K. S. Choi, S. Park, and S. Chang, *Sens. Actuators, B*, **238**, 871 (2017).
31. Y. Kwon, H. Kim, S. Lee, I. Chin, T. Seong, W. I. Lee, and C. Lee, *Sens. Actuators, B*, **173**, 441 (2012).
32. S. Hung, C. Chang, C. Hsu, B. H. Chu, C. F. Lo, C. Hsu, S. J. Pearton, M. R. Holzworth, P. G. Whiting, N. G. Rudawski, K. S. Jones, A. Dabiran, P. Chow, and F. Ren, *Int. J. Hydrogen Energy*, **37**, 13783 (2012).
33. S. Jang, J. Kim, and K. H. Baik, *J. Electrochem. Soc.*, **163**, B456 (2016).
34. K. H. Baik, J. Kim, and S. Jang, *ECS Trans.*, **72**, 23 (2016).
35. S. Jang, P. Son, J. Kim, S. Lee, and K. H. Baik, *Sens. Actuators, B*, **222**, 43 (2016).
36. K. H. Baik, H. Kim, S. Lee, E. Lim, S. J. Pearton, F. Ren, and S. Jang, *Appl. Phys. Lett.*, **104**, 072103 (2014).
37. H. Kim, W. Lim, J. Lee, S. J. Pearton, F. Ren, and S. Jang, *Sens. Actuators, B*, **164**, 64 (2012).
38. A. Zhong, T. Sasaki, and K. Hane, *Sens. Actuators, A*, **209**, 52 (2014).
39. W. Lim, J. S. Wright, B. P. Gila, J. L. Johnson, A. Ural, T. Anderson, F. Ren, and S. J. Pearton, *Appl. Phys. Lett.*, **93**, 72109 (2008).
40. K. H. Baik, J. Kim, and S. Jang, *Sens. Actuators, B*, **238**, 462 (2017).
41. H. Kim, W. Lim, J. Lee, S. J. Pearton, F. Ren, and S. Jang, *Sens. Actuators, B*, **164**, 64 (2012).
42. S. J. Pearton, F. Ren, Y. Wang, B. H. Chu, K. H. Chen, C. Y. Chang, W. Lim, J. Lin, and D. P. Norton, *Prog. Mater. Sci.*, **55**, 1 (2010).
43. B. S. Kang, H. T. Wang, F. Ren, and S. J. Pearton, *J. Appl. Phys.*, **104**, 031101 (2008).
44. R. Wu, D. Lin, M. Yu, M. H. Chen, and H. Lai, *Sens. Actuators, B*, **178**, 185 (2013).
45. Y. Wang, F. Ren, W. Lim, S. J. Pearton, K. H. Baik, S. Hwang, Y. G. Seo, and S. Jang, *Curr. Appl. Phys.*, **10**, 1029 (2010).
46. H. Kim and S. Jang, *Curr. Appl. Phys.*, **13**, 1746 (2013).
47. J. Kim, K. Baik, and S. Jang, *Curr. Appl. Phys.*, **16**, 221 (2016).
48. E. M. Cordi and J. L. Falconer, *Appl. Catal. A*, **15**, 179 (1997).
49. R. K. Joshi and F. E. Kruis, *Appl. Phys. Lett.*, **89**, 153116 (2006).
50. I. E. Wachs and R. J. Madix, *Appl. Surface Sci.*, **1**, 303 (1978).
51. S. C. Hung, C. W. Chen, C. Y. Shieh, G. C. Chi, R. Fan, and S. J. Pearton, *Appl. Phys. Lett.*, **98**, 223504 (2011).
52. C. Lo, Y. Xi, L. Liu, S. J. Pearton, S. Doréc, C. Hsu, A. M. Dabiran, P. P. Chow, and F. Ren, *Sens. Actuators, B*, **176**, 708 (2013).